

brain calcium channel subunits cDNAs (N-type: $\alpha_{1B} + \alpha_{2\delta-1} + \beta_{1b}$ subunits; L-type: $\alpha_{1C} + \alpha_{2\delta-1} + \beta_{1b}$ subunits). After incubation for 24–72 h, whole cell current recordings were performed with barium as the charge carrier as previously described.⁹ Currents were typically elicited from a holding potential of -100 mV to the peak of current–voltage relation for each channel type. For each calcium channel subtype each compound was examined for blockade by patch clamp analysis on between 3 and 5 cells.

We began by testing the potency of flunarizine and lomerizine against the cloned N-type calcium channel exogenously expressed in HEK cells and found that they both potently inhibited functional N-type channels (estimated IC_{50} values of 0.08 and 0.09 μ M, respectively; Table 1). However, their inhibitory activities against L-type channels was also high, providing only a 1.7–3.9-fold ratio of selectivity over the two types of high voltage-activated calcium channels (Table 1). A major direction of the SAR optimization was to decrease L-type activity while maintaining the high affinity for N-type calcium channel blockade.

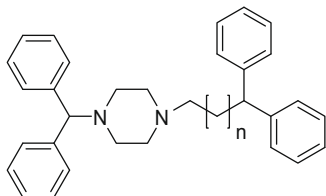
We hypothesized that the benzhydrylpiperazine and trimethoxybenzylpiperazine moieties, respectively, could be acting as selectivity elements. With this in mind, we designed and synthesized a series of compounds replacing the cinnamyl portion in flunarizine. We first examined the effect of the methylene spacer between the piperazine and the benzhydryl group (Table 2). Further, we investigated the effect on N-type calcium channel activity and selectivity by changing the amine into an amide (Table 3). The SAR studies of these chemical series were guided by the whole cell patch clamp analysis of the functional blockade of N-type and L-type channels expressed in HEK cells.

Table 2 shows that the benzhydrylpiperazine backbone with a benzhydryl group on the right hand side resulted in compounds with a significantly poorer degree of N-type blockade (compounds **1a–1e**) compared with either parent compounds. Varying the length of the linker between the benzhydryl and the piperazine core resulted in a 10-fold range of N-type affinities suggesting that linker length nonetheless contributed to N-type blocking affinity.

Table 1
Blocking activities of flunarizine and lomerizine against N-type and L-type calcium channels

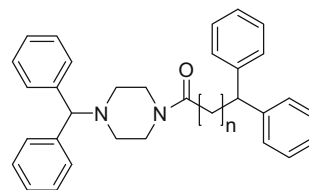
Compound	N-type Est. IC_{50} (μ M)	L-type Est. IC_{50} (μ M)	L/N ratio
Flunarizine	0.08	0.31	3.9
Lomerizine	0.09	0.15	1.7

Table 2
N-type calcium channel blocking activities for compounds **1a–1e**



Compound	<i>n</i>	N-type Est. IC_{50} (μ M)
1a	0	>50
1b	1	5
1c	2	6
1d	3	20
1e	4	50

Table 3
N-type and L-type calcium channel blocking activities for compounds **2a–2e**



Compound	<i>n</i>	N-type Est. IC_{50} (μ M)	L-type Est. IC_{50} (μ M)	L/N ratio
2a	0	>50	NA	—
2b (NP118809)	1	0.11	12.2	111
2c	2	23	NA	—
2d	3	>50	NA	—
2e	4	50	NA	—

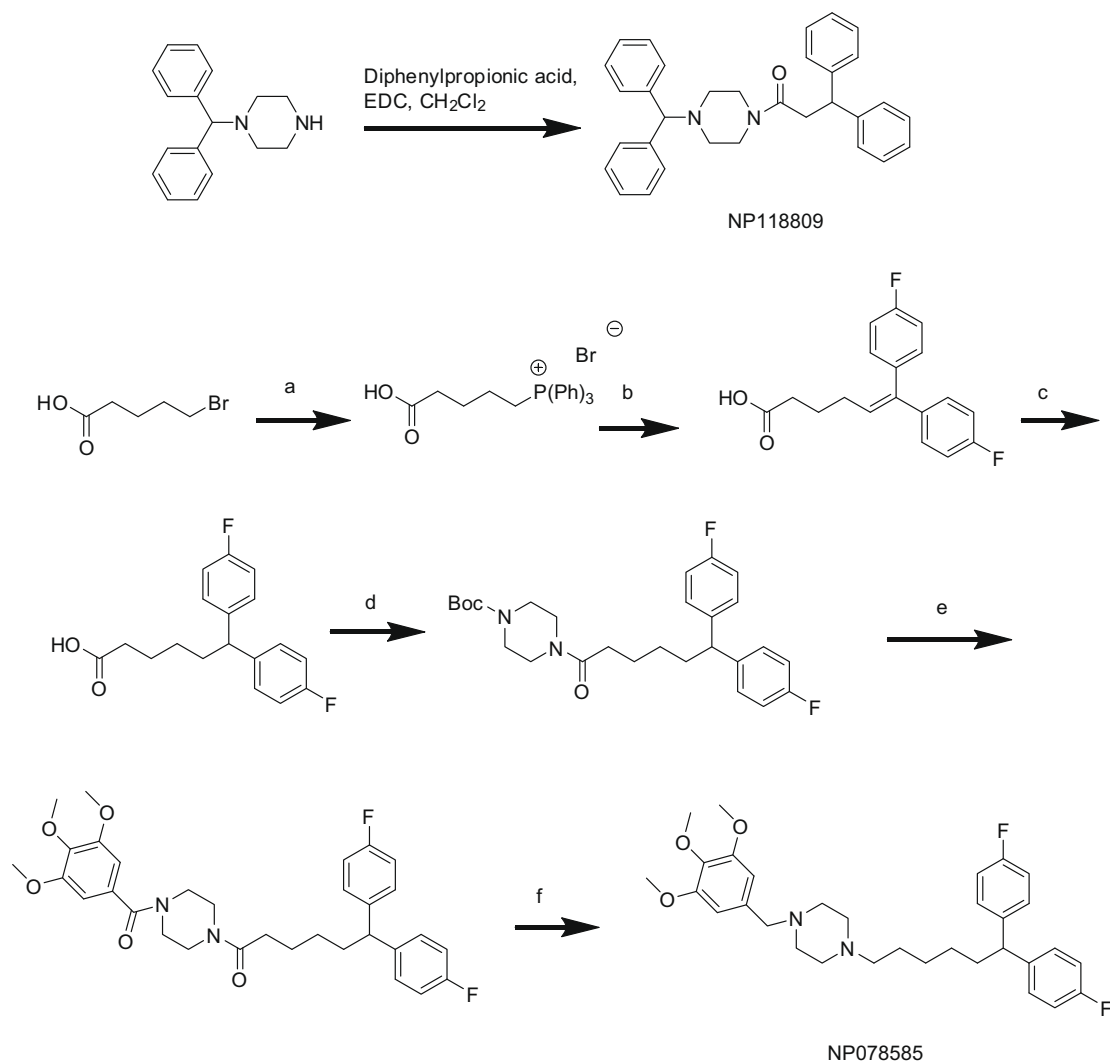
Table 3 shows that the introduction of an amide into the right hand linker was also generally unfavorable compared to the parent compounds. A notable exception to this was compound **2b** (NP118809; see Scheme 1) with a total linker length of 3 carbons ($n = 1$) and which exhibited approximately a 500-fold increased N-type channel blockade compared to compounds in this series with linkers either shorter ($n = 0$, **2a**) or longer ($n = 2–4$, **2c–e**). Examination of the effect of NP118809 on functional L-type calcium channel activity showed that this compound was approximately 111-fold more selective for N-type channels.

To probe the effect of bioisosteric replacement of carbon on the NP118809 linker, we examined the bioisosteric potential of 3,3-diphenylpropan-1-one bound to the piperazine core, while maintaining the benzhydryl moiety on the opposite side of molecule (Scheme 2). This modification allowed the maximum conservation of the polarity and geometry of the NP118809 (Table 4). While compound **3a** maintained favorable inhibitory activity for N-type channels (est. $IC_{50} = 0.15$ μ M) compared to that of NP118809, the N-type:L-type selectivity profile was significantly lower (12-fold). Further exploration on the linker with compounds **3b–3c** showed a trend toward decreased N-type channel blocking affinity (Table 4).

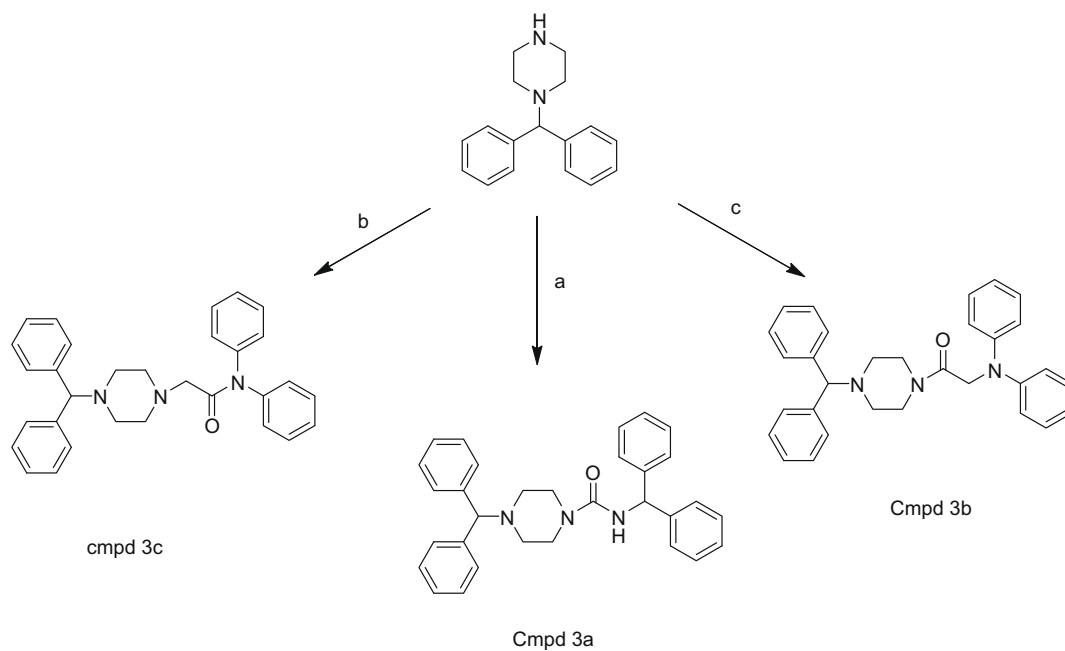
Examination of a series of derivatives focused around the lomerizine-based trimethoxybenzylpiperazine moiety resulted in compounds with a generally high degree of N-type channel blockade. Unlike that for the flunarizine-based series, a longer linker to the benzhydryl group (six carbons total length) did not seem to be deleterious. Furthermore, there was little change in N-type affinity regardless of whether an amide was included in the linker on either side of the piperazine core (Tables 5 and 6). In particular, compound **4a** (NP078585; see Scheme 1) exhibited potent N-type channel functional blockade (est. $IC_{50} = 0.11$ μ M). Examination of the effect of NP078585 on L-type calcium channels showed that this compound was approximately 25-fold more selective for N-type channels (Table 5).

Replacement of the trimethoxybenzyl with cinnamyl moiety was studied without changing the chain linker lengths (Table 6). Compound **5a** had the closest N-type potency compared to NP078585 (est. $IC_{50} = 0.05$ μ M) but possessed a lower selectivity ratio of L-type to N-type blockade (~ 7.8 -fold). The other derivatives in this series all exhibited sub-micromolar N-type channel affinities but again with no improvement over NP078585 in the L-type to N-type selectivity ratio (Table 6).

The two compounds demonstrating high affinity for the N-type channel together with the best selectivity over L-type calcium channels were selected for pharmacokinetic profiling. Examination of pharmacokinetics and oral bioavailability showed that in rats NP078585 was absorbed relatively rapidly ($T_{max} = 1.0$ h), elimi-

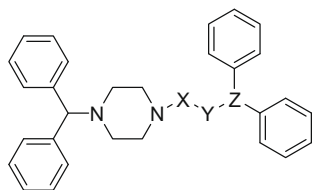


Scheme 1. Reagents and conditions: (a) PPh_3 , CH_3CN , reflux; (b) LiHMDS , -78°C , benzophenone; (c) MeOH , H_2 , 5% Pd/C , 50 psi; (d) Boc-piperazine, EDC; (e) 25% TFA, 3,4,5-trimethoxybenzoylchloride, K_2CO_3 ; (f) LiAlH_4 , THF.



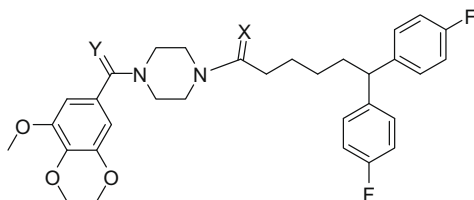
Scheme 2. Reagents and conditions: (a) diphenylmethyl isocyanate, rt; (b) 2-bromo-*N,N*-diphenylacetamide, NaHCO_3 , CH_3CN , reflux; (c) 2-(diphenylamino)acetic acid, EDC, DMAP.

Table 4
N-type and L-type calcium channel blocking activities for compounds **3a–3c**



Compound	X	Y	Z	N-type Est. IC ₅₀ (μM)	L-type Est. IC ₅₀ (μM)	L/N ratio
3a	CO	NH	CH	0.15	1.84	12
3b	CO	CH	N	6.61	NA	—
3c	CH	CO	N	0.26	NA	—

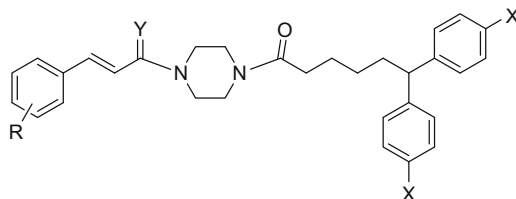
Table 5
N-type and L-type calcium channel blocking activities for compounds **4a–4c**



Compound	Y	X	N-type Est. IC ₅₀ (μM)	L-type Est. IC ₅₀ (μM)	L/N ratio
4a (NP078585)	H	H	0.11	2.8	12
4b	O	O	0.54	NA	—
4c	H	O	0.19	NA	—

nated moderately slowly ($t_{1/2} = 4.5$ h) and possessed an oral bioavailability of 20% (Table 7). The mean volume of distribution for **NP078585** following intravenous administration (11,693 ml/kg) was in excess of the calculated total body water in the rat suggesting that **NP078585** was widely distributed outside of plasma and/or bound to plasma proteins. **NP118809** exhibited both acceptable absorption ($T_{max} = 2.3$ h) and half-life ($t_{1/2} = 2.1$ h) characteristics and a mean oral bioavailability of 30%. Similar to that for **NP078585**, the volume of distribution of **NP118809** (5787 ml/kg)

Table 6
N-type and L-type calcium channel blocking activities for compounds **5a–5h**



Compound	Y	X	R	N-type Est. IC ₅₀ (μM)	L-type Est. IC ₅₀ (μM)	L/N ratio
5a	H	H	H	0.05	0.39	8
5b	H	<i>p</i> -F	H	0.09	0.12	1.3
5c	H	H	H	0.12	0.33	2.8
5d	H	H	<i>p</i> -Methoxy	0.19	NA	—
5e	O	H	<i>p</i> -Methoxy	0.09	0.25	2.8
5f	H	H	1,3-Dioxole	0.19	NA	—
5g	O	H	1,3-Dioxole	0.13	0.74	5.7
5h	O	H	<i>p</i> -Amino	0.15	0.83	5.5

was suggestive of a high degree of protein binding and/or distribution outside of plasma.

Based upon their combined in vitro and pharmacokinetic properties **NP078585** and **NP118809** were subject to in vivo assay in the rat formalin model inflammatory pain.¹⁰ Figure 2 shows that upon intraperitoneal (ip) administration both **NP118809** and **NP078585** (25 mg/kg) both exhibited significant analgesic activity in the phase IIA portions of the rat formalin model.

In order to further refine the preclinical profiles of the two candidate molecules their off-target interactions with the hERG potassium channel was examined by whole cell patch clamp analysis of HEK cells stably expressing hERG. A single 1 μM dose application of **NP078585** was found to significantly block hERG currents ($98.7 \pm 0.2\%$, $n = 3$) suggesting the potential for cardiovascular liability for this agent. Contrastingly, an initial single test dose test of **NP118809** (1 μM) resulted in only partial blockade of hERG currents ($24.8 \pm 0.3\%$, $n = 3$). Subsequently, a dose–response profile on hERG tail currents was determined for **NP118809**. Figure 3 shows the estimated IC₅₀ of **NP118809** for the hERG channel extrapolated from the concentration-dependent inhibition curve = 7.4 μM. As such, **NP118809** would not be considered a potent blocker of the hERG potassium channel.

Further examining **NP118809** at a concentration of 10 μM for off-target activity using a radioligand binding displacement screen of 112 ion channel, receptor and other signaling targets (MDS Pharma Services; <http://discovery.mdsp.com>) resulted in >50% displacement of radioligand from only four targets: L-type calcium channel, cannabinoid CB₁, μ opiate receptor and voltage-gated sodium channel. Subsequent secondary screens for possible functional interactions against these targets by **NP118809** using representative tissue assays (MDS Pharma Services) showed no significant agonism or antagonism (>50%) at a higher test concentration of 30 μM. That there was no observed physiological effect of **NP118809** on L-type channel function in a guinea pig model of atrial inotropy while we determined an IC₅₀ ~ 12 μM against the L-type channel by electrophysiological assessment is likely reflective of the highly state-dependent nature of **NP118809** channel blockade (data not shown). Voltage- and frequency-dependent blockade would favor drug interaction with a subset of channels under native conditions and are predicted to be important factors towards maximizing the therapeutic window of ion channel blockers in vivo.¹¹

In summary, SAR studies around the flunarizine and lomerizine diphenylmethylpiperazine backbones produced a series of high

Table 7
Mean pharmacokinetic parameters in rat plasma following single oral or intravenous dosing for **NP078585** and **NP118809**

Compound/route	Dose (mg/kg)	C _{max} (ng/ml)	T _{max} (h)	AUC ₍₀₋₈₎ (ng h/ml)	AUC _(t) (ng h/ml)	t _{1/2} (h)	V _{dss} (ml/kg)	CL/F (ml/h kg)	F (%)
NP078585 intravenous	2	462 (182)	NA	725 (104)	975 (192)	5.0 (1.1)	11693 (1360)	2111 (449)	NA
NP078585 oral	10	173 (64)	1.0 (0.0)	753 (292)	1021 (269)	4.5 (2.0)	NA	10204 (2331)	21 (5.5)
NP118809 intravenous	2	771 (95)	NA	715 (171)	761 (169)	3.3 (1.2)	5787 (2345)	2730 (680)	NA
NP118809 oral	10	235 (94)	2.3 (1.5)	999 (386)	1136 (469)	2.1 (0.5)	NA	9868 (3969)	30 (12.3)

Data are presented as mean (standard error in brackets).

AUC₍₀₋₈₎: Area under the plasma concentration versus time curve from time zero to 8 h post-dose.

AUC_(t): Area under the plasma concentration versus time curve from time zero to infinity.

C_{max}: The highest observable concentration.

T_{max}: Time to C_{max}.

CL/F: Plasma clearance.

V_{dss}: Apparent volume of distribution.

t_{1/2}: Terminal elimination half-life.

F: Oral bioavailability.

NA: Not applicable.

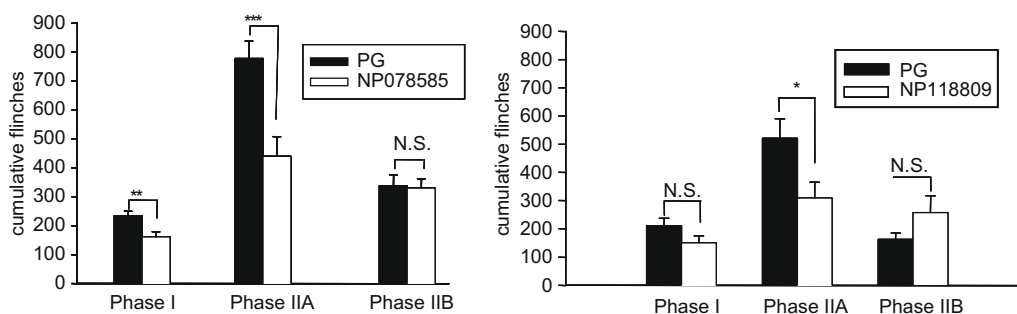


Figure 2. Efficacy of **NP078585** and **NP118809** in the rat formalin model of inflammatory pain. Compounds were administered at a dose of 25 mg/kg ip **NP078585** $n = 26$ animals, **NP118809** $n = 24$ animals. Statistical significance $^* p < 0.01$; $^{***} p < 0.001$.

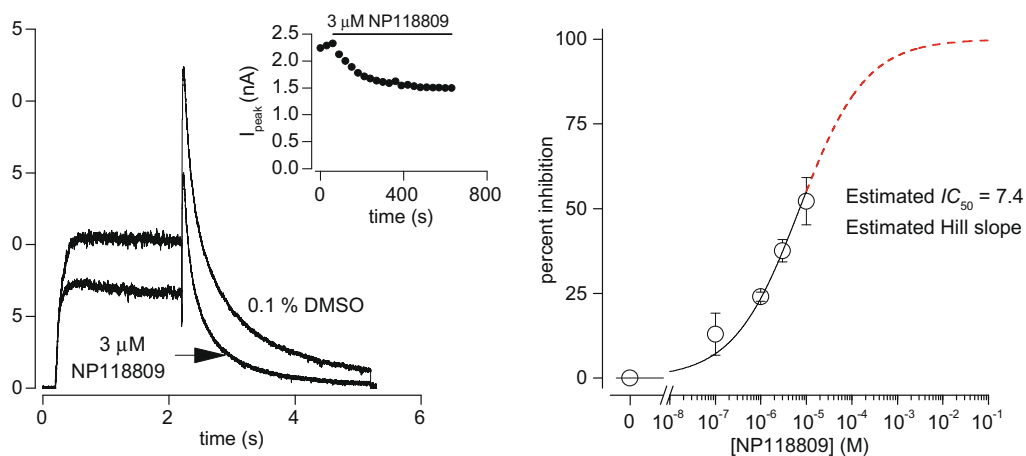


Figure 3. Concentration-dependent inhibition of the hERG potassium channel by **NP118809**. (A) hERG tail currents recorded in the presence of 0.1% DMSO (control) and after application of 3 μ M **NP118809**. Inset shows the rate of inhibition of the tail current by 3 μ M **NP118809** from the same cell. (B) Concentration-dependent inhibition of the peak hERG channel tail currents by **NP118809**. The concentration-dependent inhibition curve was generated by using the mean data obtained for 0.1, 1, 3 and 10 μ M **NP118809** (solid line) and extrapolated to 100% inhibition (dash line). Data are the mean of 4 values \pm standard error for each concentration applied. Data was analyzed and fitted using OriginPro v.7 software. To obtain the IC_{50} and Hill slope coefficient (n_H) the concentration–response curve was fitted with a logistic equation of:

$$y = \max \left[1 - \frac{1}{1 + \left(\frac{\text{drug}}{IC_{50}} \right)^{n_H}} \right]$$

affinity N-type calcium channel blockers (<200 nM IC_{50} s) that exhibit a significant degree of selectivity (25–111-fold) over the closely related L-type channel. **NP078585** and **NP118809** were discovered as N-type calcium channel antagonists that exhibit strong analge-

sic activity in an inflammatory rat model. Both compounds exhibit suitable pharmacokinetic characteristics for animal testing although **NP118809** appears to be the more favorable preclinical candidate based upon its lower off-target affinity to the hERG

potassium channel and lack of significant interaction against 112 additional molecular targets. Some relevant experimental details have already been published in another form.¹²

Acknowledgments

Work in the laboratories of T.P.S. and G.W.Z. is supported by the Canadian Institutes of Health Research. T.P.S. a Canada Research Chair in Biotechnology and Genomics-Neurobiology. G.W.Z. is a Scientist of the Alberta Heritage Foundation for Medical Research and is also supported by a Canada Research Chair in Molecular Neurobiology.

References and notes

1. Gribkoff, V. K.; Starrett, J. E. *Expert Opin. Pharmacother.* **1999**, *1*, 61.
2. (a) Catterall, W. A. *Annu. Rev. Cell Dev. Biol.* **2000**, *16*, 521; (b) Cox, B.; Denyer, J. C. *Expert Opin. Ther. Patents* **1998**, *8*, 1237; (c) Elmsile, K. S. J. *Neurosci. Res.* **2004**, *75*, 733.
3. Snutch, T. P.; Peloquin, J.; Mathews, E.; McRory, J. Molecular Properties of Voltage-Gated Calcium Channels. In *Voltage-Gated Calcium*; Zamponi, G., Ed.; Landes Bioscience, 2005; pp 61–94.
4. (a) Kerr, L. M. et al *Eur. J. Pharmacol.* **1998**, *146*, 181; (b) Dubel, S. J. et al *Proc. Natl. Acad. Sci. U.S.A.* **1992**, *89*, 5058; (c) Westenbroek, R. E. et al *Neuron* **1992**, *9*, 1099; (d) Dunlap, K.; Luebke, J. I.; Turner, T. J. *Trends Neurosci.* **1995**, *18*, 89.
5. (a) Hu, L.-Y. et al *Bioorg. Med. Chem. Lett.* **1999**, *9*, 907; (b) Hu, L.-Y. et al *Bioorg. Med. Chem. Lett.* **1999**, *9*, 1121; (c) Knutsen, L. J. S. et al *Bioorg. Med. Chem. Lett.* **2007**, *17*, 662; (d) Shoji, Masataka et al *Bioorg. Med. Chem. Lett.* **2006**, *14*, 5333.
6. (a) Staats, P. S. et al *J. Am. Med. Assoc.* **2004**, *291*, 63; (b) Jain, K. K. *Expert Opin. Invest. Drugs* **2000**, *9*, 2403; (c) Bowersox, S.; Tich, N.; Mayo, M.; Luther, R. *Drugs Future* **1998**, *23*, 152.
7. (a) Cohan, S. L.; Redmond, D. J.; Chen, M.; Wilson, D.; Cyr, P. J. *Cereb. Blood Flow Metab.* **1993**, *13*, 947; (b) Pauwels, P. J.; Leysen, J. E.; Janssen, P. A. J. *Life Sci.* **1991**, *48*, 1881.
8. Hara, H.; Morita, T.; Sukamoto, T.; Cutrer, F. M. *CNS Drug Rev.* **1995**, *1*, 204.
9. Bourinet, E. et al *Nature Neurosci.* **1999**, *2*, 407.
10. (a) Dubuisson, D.; Dennis, S. G. *Pain* **1977**, *4*, 161; (b) Malmberg, A. B.; Yaksh, T. L. *J. Neurosci.* **1994**, *14*, 4882.
11. Snutch, T. P. *NeuroRx* **2005**, *2*, 662.
12. Snutch, T. P.; Zamponi, G. W. U.S. Patent, 7,064, 128 B2, 2006.; Snutch, T.P. U.S. Patent 6,387,897, 2002.